Focal-adhesion targeting links caveolin-1 to a Rac1-degradation pathway

Micha Nethe[1], Eloise C. Anthony[1], Mar Fernandez-Borja[1], Rob Dee[2], Dirk Geerts[3], Paul J. Hensbergen[4], André M. Deelder[4], Gudula Schmidt[5] and Peter L. Hordijk[1,*]

[1]Department of Molecular Cell Biology, [2]Department of Experimental Immunohematology, Sanquin Research and Landsteiner Laboratory, Academic Medical Center, University of Amsterdam, Plesmanlaan 125, 1066 CX Amsterdam, The Netherlands
[3]Department of Human Genetics, Academic Medical Center, University of Amsterdam, Plesmanlaan 125, 1066 CX Amsterdam, The Netherlands
[4]Biomolecular Mass Spectrometry Unit, Department of Parasitology, Leiden University Medical Center, Albinusdreef 2, 2333 ZA Leiden, The Netherlands
[5]Institut für Experimentelle und Klinische Pharmakologie und Toxikologie, Albert-Ludwigs-Universität Freiburg, Albert-Strasse 25, 79104 Freiburg, Germany
*Author for correspondence (p.hordijk@sanquin.nl)

Accepted 22 March 2010
Journal of Cell Science 123, 1948-1958

doi:10.1242/jcs.062919

Summary

Directional cell migration is crucially dependent on the spatiotemporal control of intracellular signalling events. These events regulate polarized actin dynamics, resulting in protrusion at the front of the cell and contraction at the rear. The actin cytoskeleton is regulated through signalling by Rho-like GTPases, such as RhoA, which stimulates myosin-based contractility, and CDC42 and Rac1, which promote actin polymerization and protrusion. Here, we show that Rac1 binds the adapter protein caveolin-1 (Cav1) and that Rac1 activity promotes Cav1 accumulation at Rac1-positive peripheral adhesions. Using Cav1-deficient mouse fibroblasts and depletion of Cav1 expression in human epithelial and endothelial cells mediated by small interfering RNA and short hairpin RNA, we show that loss of Cav1 induces an increase in Rac1 protein and its activated, GTP-bound form. Cav1 controls Rac1 protein levels by regulating ubiquitylation and degradation of activated Rac1 in an adhesion-dependent fashion. Finally, we show that Rac1 ubiquitylation is not required for effector binding, but regulates the dynamics of Rac1 at the periphery of the cell. These data extend the canonical model of Rac1 inactivation and uncover Cav1-regulated polyubiquitylation as an additional mechanism to control Rac1 signalling.

Key words: Rac1GTPase, Caveolin-1, Adhesion, Ubiquitylation

Introduction

Directional cell migration is crucially dependent on the spatiotemporal regulation of intracellular signalling events. These events control cytoskeletal dynamics, providing both driving force at the front of the cell and contraction at the rear. The actin cytoskeleton is central to these processes and is regulated through signalling by Rho-like small GTPases such as RhoA, which stimulates myosin-based contractility, and CDC42 and Rac1, which promote actin polymerization and cell protrusion (Ridley et al., 2003; Vicente-Manzanares et al., 2005).

Like most other small GTPases, Rho family members act as molecular switches, cycling between an active, GTP-bound state and an inactive, GDP-bound state. These transitions are stimulated by guanine nucleotide exchange factors (GEFs) and GTPase-activating proteins (GAPs) (Bernards and Settleman, 2004; Bos et al., 2007; Rossman et al., 2005). Additionally, Rho GTPases cycle between the plasma membrane and the cytosol, where they are bound to RhoGDI (Rho guanine nucleotide dissociation inhibitor) (DerMardirossian and Bokoch, 2005; Dovas and Couchman, 2005). GEF-mediated GTPase activation and dissociation from RhoGDI takes place at cellular membranes, as most GEFs associate with membranes through pleckstrin homology (PH)-domain-mediated binding to phosphatidylinositol lipids (Bos et al., 2007; Rossman et al., 2005). Although GTP loading is crucial to GTPase function, GTPase cycling (i.e. controlled GTPase inactivation) is considered equally important for efficient signal transduction. Accumulating evidence suggests that, in addition to GAP-stimulated GTP hydrolysis, other mechanisms exist that serve to turn off GTPase signalling.

Activation of Rac1 and RhoA by bacterial toxins such as cytotoxic necrotizing factor 1 (CNF1) leads, after 4-6 hours, to proteasome-mediated degradation (Munro and Lemichez, 2005; Pop et al., 2004). Thus, cells possess endogenous mechanisms to degrade activated GTPases, representing a third level of regulation, in addition to membrane translocation and GTP loading and hydrolysis. Degradation of RhoA occurs in a polarized fashion and requires the E3 ubiquitin ligase Smurf1 (Wang et al., 2003). For Rac1, it has been shown that activated mutants are more susceptible to ubiquitylation and degradation, and that this pathway can be activated by receptor agonists, as demonstrated for hepatocyte growth factor (HGF) in epithelial MDCK cells (Doye et al., 2002; Lynch et al., 2006; Pop et al., 2004). However, the cellular mechanisms that control the degradation of activated Rac1 are unknown.

Here, we show that the membrane-associated adapter protein caveolin-1 (Cav1) is part of a signalling pathway that regulates the ubiquitylation and degradation of Rac1. Rac1 associates, through its hypervariable C-terminal domain, with the scaffolding domain of Cav1 in an adhesion-stimulated fashion. Interestingly, Rac1 activation recruits Cav1 to peripheral focal adhesions, colocalizing with endogenous Rac1, paxillin and β1 integrins. Cav1, in turn, regulates Rac1 protein levels by regulating the polyubiquitylation and degradation of Rac1 in an adhesion-dependent fashion, controlling cell polarity, spreading and migration. Together, our

Journal of Cell Science

findings show that Cav1 is part of a negative-feedback loop that promotes directional cell migration by controlling the degradation of activated Rac1.

Results

The caveolin-1 scaffolding domain associates with the C terminus of Rac1

We recently identified Cav1 as a Rac1-binding protein, in the course of our studies on the intercellular adhesion molecule 1 (ICAM-1)–filamin–Cav1 complex (Kanters et al., 2008). This finding is in agreement with an earlier study (Zuluaga et al., 2007) that showed Rac1 binding to immunoprecipitated Cav1 in cardiomyocytes. Using biotinylated peptides, we found that endogenous Cav1, but not Cav2, binds to the Rac1 C terminus, but does not associate with amino acids 17-32, part of the Rac1 effector domain (Fig. 1A) (Vastrik et al., 1999). Peptides encoding the C termini of RhoA and RhoC also bind to Cav1, complementing published data (Gingras et al., 1998; Lin et al., 2005), but the C termini of CDC42, RhoG, Rac2 and RhoB do not (Fig. 1A). Bacterially purified, full-length GST-Rac1, but not GST-Rac1ΔC (which lacks the Rac1 C terminus), binds endogenous Cav1 (Fig. 1B), indicating that the Rac1 C terminus is both necessary and sufficient for Cav1 binding.

Tyrosine phosphorylation of Cav1 on Tyr14 (pYCav1) has been implicated in Cav1-mediated signalling and in its internalization (del Pozo et al., 2005). Levels of tyrosine-phosphorylated Cav1 in cells are on the order of 1% only and we therefore induced higher levels of pYCav1 by treating cells with pervanadate (Grande-Garcia et al., 2007). This pYCav1, detected using a pY14Cav1-specific antibody, associates with the C terminus of Rac1 (Fig. 1C), indicating that Cav1 phosphorylation does not interfere with its interaction with Rac1. Conversely, a mutant of Cav1 that cannot be phosphorylated on residue 14, Y14FCav1, also associates with the Rac1 C terminus (Fig. 1D). Together, these data suggest that tyrosine phosphorylation of Cav1 does not play a regulatory role in the interaction with Rac1.

The Rac1 C-terminal domain comprises two binding sites for protein-protein interactions (van Hennik et al., 2003). Use of mutant peptides showed that both the proline stretch and the polybasic region are required for Rac1 binding to Cav1 (Fig. 1E,F). In this experiment, we used I1PP2A (inhibitor 1 of protein phosphatase 2) (ten Klooster et al., 2007) as a control for binding to a Rac1 C-terminal peptide in which the prolines were mutated. The relevance of this sequence to Cav1 binding was further supported by the reduced binding of Cav1 to the C terminus of Rac3, a closely related homologue of Rac1 with a C terminus that contains three consecutive proline residues, but differs by two amino acids in the polybasic region (Fig. 1E,G). In agreement with the data showing Rac1 binding to endogenous Cav1 (Fig. 1B), GST-Cav1, but not GST alone, binds to endogenous Rac1 (Fig.

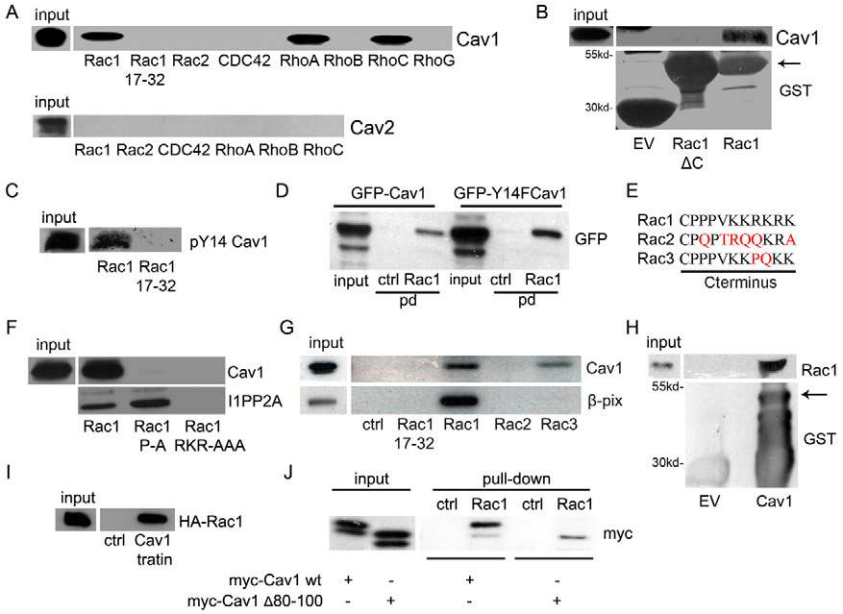

Fig. 1. Rac1 associates with Cav1. (**A**) Biotinylated peptides encoding the C-terminal domains of different Rho GTPases, fused to a transduction domain, were assayed for binding to endogenous Cav1 or Cav2 in streptavidin-based peptide pull-down assays. In addition to Rac1, the C termini of RhoA and RhoC showed binding to Cav1, but not to Cav2. (**B**) Bacterially purified full-length GST-Rac1 but not GST-Rac1ΔC, which lacks the Rac1 C-terminal domain (arrow), associates with endogenous Cav1. EV, empty vector. (**C**) HeLa cells were treated with pervanadate to induce Cav1 tyrosine phosphorylation. They were then used to analyze the binding of endogenous pY14Cav1, detected using a phospho-specific antibody, to Rac1 peptides encoding part of the effector loop (17-32) or the C terminus. (**D**) Conversely, the association of a transiently expressed, non-phosphorylatable GFP-Y14FCav1 protein was tested in a Rac1 C-terminal peptide pull down. Because this protein associates as equally well with the Rac1 C terminus as wild-type Cav1, this result shows that tyrosine phosphorylation does not regulate this interaction. (**E**) Alignment of the hypervariable C-terminal domains of Rac1, Rac2 and Rac3. (**F**) Biotinylated peptides encoding Rac1 C-terminal domains in which the proline stretch or polybasic region were changed to alanines are no longer able to bind endogenous Cav1 in HeLa cell lysates. The association with I1PP2A, which we previously described to bind the Rac1 C terminus, was included as a control. (**G**) Association with Cav1, as compared with Rac1 binding to β-Pix, was tested for the C termini of Rac1, Rac2 and Rac3. The Rac3 C-terminal domain, like Rac1, harbours a polyproline stretch and associates with Cav1. (**H**) Bacterially purified GST-Cav1 (arrow) associates with endogenous Rac1 from HeLa cell lysates. EV, empty vector. (**I**) Biotinylated cavtratin, encoding the scaffolding domain of Cav1, was used to test its binding to HA-tagged, ectopically expressed Rac1. (**J**) Myc-tagged full-length Cav1 or a Cav1Δ80-100 mutant, which lacks the scaffolding domain, were used to further map the Cav1 interaction with Rac1.

1H). Many of the protein-protein interactions described for Cav1, which binds to a series of signalling proteins (Razani et al., 2002), are mediated by the 'caveolin scaffolding domain' (CSD), which is formed by amino acids 82-101. This sequence is divergent between Cav1 and Cav2 (Razani et al., 2002). Use of cavtratin, a cell-permeable peptide encoding the Cav1 CSD, showed that this region is sufficient to mediate the Cav1-Rac1 interaction (Fig. 1I). Conversely, a myc-tagged version of Cav1 lacking the CSD (myc-Cav1Δ80-100) showed reduced binding to the Rac1 C-terminal domain (Fig. 1J). The observed residual binding could be due to additional regions, outside the scaffolding domain of Cav1, contributing to the Cav1-Rac1 association. Together, these findings show that the Cav1 CSD is necessary and sufficient for optimal association with Rac1, and that additional regions within the Cav1 protein might further promote formation of the complex.

Rac1 activation recruits endogenous caveolin-1 to peripheral focal adhesions

Subsequent analysis by immunostaining in combination with confocal microscopy showed endogenous Rac1 to predominantly

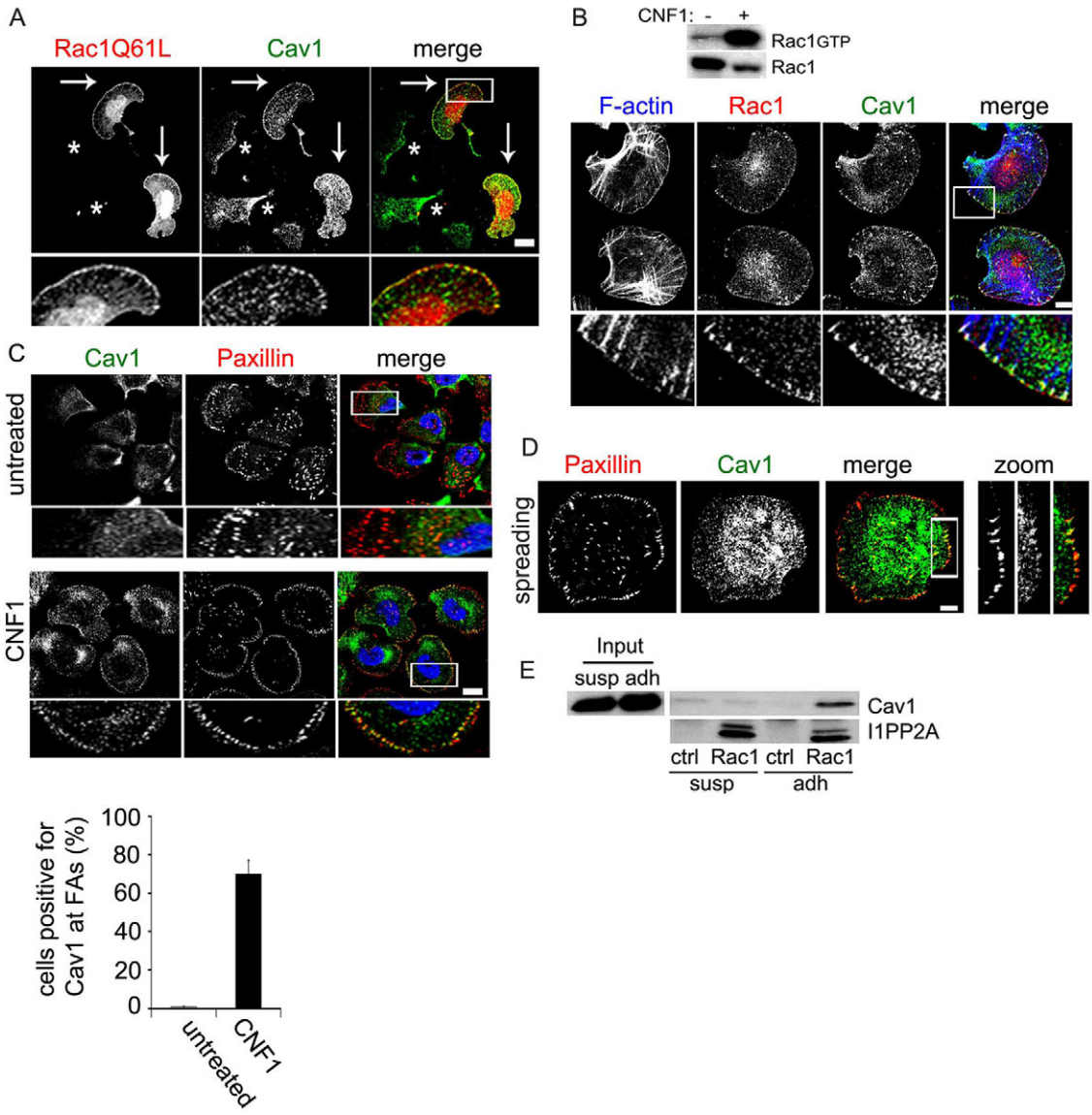

Fig. 2. Active Rac1 recruits Cav1 to peripheral FAs. (**A**) HeLa cells were transfected with myc-tagged Rac (Q61L; arrows) and stained for (co)localization of Rac1Q61L and endogenous Cav1. Scale bar: 20 µm. Untransfected cells are indicated with asterisks and close-up images are included to underscore the Rac1-Cav1 colocalization at the periphery of the cells. (**B**) Rac1 activation in control or CNF1-treated HeLa cells was analyzed by a Pak-Crib pull-down assay (upper panel), parallel to imaging the (co)localization of endogenous Rac1 and Cav1 in CNF1-treated HeLa cells. Scale bar: 10 µm. (**C**) (Co)localization of endogenous Cav1 with paxillin was analyzed by immunostaining in control and CNF1-treated HeLa cells. Scale bar: 10 µm. The bar diagram shows the percentage of cells in which Cav1 was determined to colocalize with paxillin-marked sites of adhesion upon stimulation with CNF1, as analyzed by Zen colocalization software (Zeiss) (50 cells/condition; n=3). (**D**) Immunostaining for endogenous Cav1 and paxillin following spreading of HeLa cells for 1 hour on fibronectin shows colocalization at the periphery of the cell. Scale bar: 5 µm. (**E**) Rac1 C-terminal peptide pull down from lysates of HeLa cells kept for 1 hour in suspension (susp) or plated on fibronectin (adh) was performed to test the binding to endogenous Cav1 and I1PP2A, included as a control. The Rac1-Cav1 interaction is increased in adherent cells, but absent in cells kept in suspension.

localize to membrane ruffles, to focal adhesions (FAs) and to a perinuclear compartment (supplementary material Fig. S1). Colocalization of Rac1 with endogenous Cav1, which concentrates at the contractile rear of polarized cells (supplementary material Fig. S1B,C), was limited. Antibody specificity was confirmed by analysis of Rac1 and Cav1 staining of cells transfected with the corresponding small interfering RNAs (siRNAs) (supplementary material Fig. S1A,B). Although most Cav1, endogenous and GFP tagged, was localized to the rear of polarized cells, live-cell imaging revealed a portion of the pool of GFP-Cav1 to translocate from the front of the cell towards the centre, probably on vesicles (supplementary material Movie 1 and Fig. S2E).

Interestingly, expression of an activated mutant of Rac1, Rac1Q61L, in HeLa cells induced a marked re-localization of endogenous Cav1 to Rac1Q61L-positive peripheral sites of adhesion (Fig. 2A). Similarly, activating endogenous Rac1 with CNF1 (Flatau et al., 1997; Pop et al., 2004) induced the accumulation of endogenous Cav1 at peripheral adhesions (Fig. 2B,C). Immunostaining of CNF1-treated human umbilical vein endothelial cells (HUVEC) confirmed that, in this cell type also, activation of endogenous Rac1 promotes Cav1 accumulation at FAs (supplementary material Fig. S3A). In adhesion structures, Cav1 colocalizes with endogenous Rac1, paxillin and β1 integrin (Fig. 2B,C; supplementary material Fig. S3B). Unlike Cav1, the localization of clathrin did not change upon CNF1-mediated Rac1 activation (not shown).

We did not pursue analysis of pY14Cav1 localization by immunofluorescence, as previous claims of its localization to FAs have been questioned as a result of cross-reactivity of the phospho-Cav1 antibody with phospho-paxillin (Hill et al., 2007). Alternatively, we used live-cell imaging analysis of HeLa cells co-transfected with mCherry-tagged Rac1Q61L and either GFPCav1 or GFPCavY14F. These data showed that GFPCav1Y14F is unable to colocalize with active Rac1 to sites of adhesion, suggesting that phosphorylation of Cav1 on Tyr14 is required for Cav1 localization at FAs (supplementary material Movies 2 and 3). As phosphorylation of Cav1 on Tyr14 does not appear to be required for Rac1 binding, this finding further suggests that, in addition to Rac1, other proteins further promote the localization of Cav1 at FAs.

Because Cav1 trafficking has been suggested to be microtubule (MT) dependent (Conrad et al., 1995), cells were pretreated with

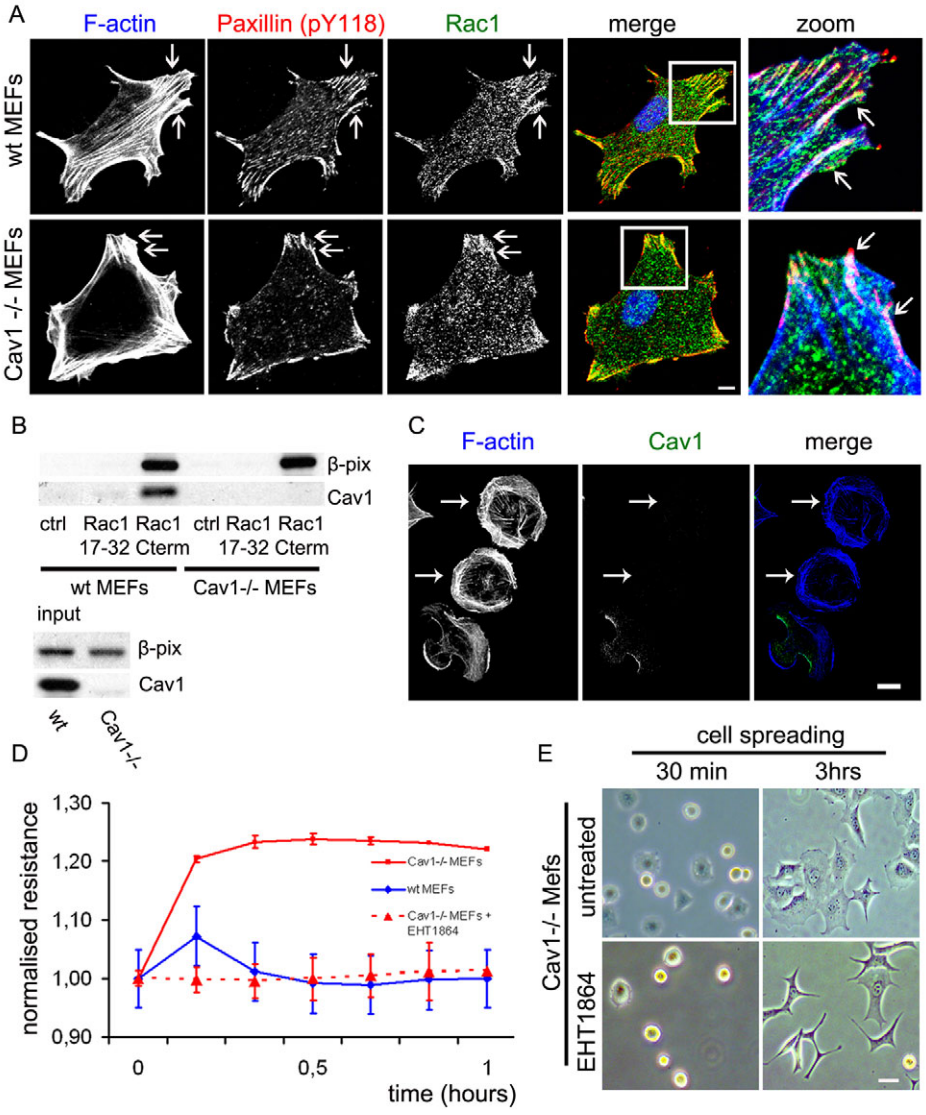

Fig. 3. Cav1 negatively regulates Rac1-mediated cell spreading, but not Rac1 targeting. (**A**) Immunostaining for endogenous Rac1 in wild-type (wt) and Cav1$^{-/-}$ MEFs shows localization of Rac1 at FAs (arrows), marked by pY118 paxillin, even in the absence of Cav1. (**B**) Rac1 C-terminal interaction with β-Pix was analyzed in the absence or presence of Cav1 using lysates from wild-type (wt) and Cav1$^{-/-}$ MEFs. The association of Rac1 with β-Pix is independent of Cav1. (**C**) Staining for F-actin underscores the cell spreading and loss of polarity of HeLa cells transfected with *Cav1* siRNA on fibronectin-coated glass coverslips. Scale bar: 20 µm. The lower polarized cell in which Cav1 expression is not reduced serves as a positive control. (**D**) Cell spreading of wild-type (wt) and Cav1$^{-/-}$ MEFs in the presence or absence of the Rac1 inhibitor EHT1864 (50 µM) was analyzed by ECIS on fibronectin-coated gold electrodes and depicted as normalized resistance. (**E**) Phase-contrast images of Cav1$^{-/-}$ MEFs spread on fibronectin for 30 minutes or 3 hours with or without EHT1864 (50 µM). Scale bar: 20 µm. These data show that the increased spreading in the Cav1$^{-/-}$ MEFs is Rac1 dependent.

the MT-disrupting agent nocodazole prior to treatment with CNF1 to activate endogenous Rac1. In the absence of CNF1 treatment, nocodazole did not induce Cav1 relocalization to peripheral adhesions (not shown). CNF1 treatment of nocodazole-treated cells induced endogenous Cav1 to relocalize to the cellular periphery, which shows that this effect is independent of MTs (supplementary material Fig. S3C).

CNF1 also mediates activation of RhoA (Schmidt et al., 1997), which, together with its downstream effector ROCK (Rho-associated, coiled-coil-containing protein kinase), is involved in the formation of FAs (Bershadsky et al., 2006). To test whether RhoA-ROCK signalling is required for the targeting of Cav1 to peripheral FAs, we treated cells with CNF1 in the presence of the ROCK inhibitor Y27632. Under these conditions, CNF1 induces the formation of a rim of paxillin-positive small adhesions at the periphery of the cells, with a marked loss of central FAs (supplementary material Fig. S3D). However, the CNF1-induced concentration of Cav1 at these peripheral adhesions was not impaired (supplementary material Fig. S3D). These data suggest that ROCK does not mediate the CNF1-induced accumulation of Cav1. Because activation of RhoA by nocodazole-induced MT depolymerization (Enomoto, 1996) also did not induce relocalization of Cav1 (not shown), the Rho-ROCK pathway appears not to be required for the targeting of Cav1 to peripheral adhesions. This is further supported by the expression of an activated mutant of RhoA that did not induce recruitment of Cav1 to FAs, despite induction of abundant actin stress fibers. Similarly, expression of activated CDC42, another CNF1 target, also did not induce recruitment of Cav1 (supplementary material Fig. S1D,E). These data are in good agreement with the notion that CNF1 induces a Rac1, rather than a CDC42 or RhoA, phenotype.

Finally, activation of endogenous Rac1 by seeding cells on fibronectin (Price et al., 1998) also induced accumulation of Cav1 at paxillin-positive peripheral FAs (Fig. 2D). In line with these results, we found cell adhesion to fibronectin to promote the Rac1 C-terminal interaction with Cav1 (Fig. 2E). Thus, cell adhesion promotes both the Rac1-Cav1 interaction and the accumulation of Cav1 at peripheral adhesions.

Rac1-driven recruitment of Cav1 is part of a negative-feedback loop

To investigate whether Rac1 acts upstream of Cav1 at FAs, (co)localization of endogenous Rac1, β-Pix and paxillin pY118 was studied by confocal microscopy in mouse embryonic fibroblasts (MEFs) genetically deficient for Cav1 ($Cav1^{-/-}$). As endogenous Rac1 (co)localizes with pY118 paxillin at peripheral sites of adhesion in $Cav1^{-/-}$ MEFs, the targeting of Rac1 towards FAs appears to be independent of Cav1 (Fig. 3A). Likewise, Rac1 localization to the ends of actin stress fibers was also unaffected in HeLa cells transfected with *Cav1* siRNA (supplementary material Fig. S4B) (Beardsley et al., 2005). Finally, the interaction of Rac1 with β-Pix, as well as their co-localization, which we previously showed to drive Rac1 targeting to FAs, was unaffected in $Cav1^{-/-}$ MEFs (Fig. 3B; supplementary material Fig. S4A) (ten Klooster et al., 2006). These data indicate that Rac1 acts upstream of Cav1 at a step downstream of β-Pix-mediated targeting of Rac1 to FAs.

As both $Cav1^{-/-}$ MEFs and HeLa cells transfected with *Cav1* siRNA showed a loss of polarity, we tested whether Cav1 controls integrin-mediated, Rac1-dependent cell spreading (Fig. 3A,C; supplementary material Fig. S4A,B,G,H). Real-time analysis of cell spreading of wild-type and $Cav1^{-/-}$ MEFs on fibronectin-coated ECIS electrodes (ten Klooster et al., 2006) showed that, similar to HeLa cells transfected with *Cav1* siRNA, depletion of Cav1 increases cell spreading (Fig. 3D; supplementary material Fig. S4E). Phase-contrast imaging of $Cav1^{-/-}$ MEFs, seeded for one hour on fibronectin, showed increased cell spreading (supplementary material Fig. S4C). This was similar to the effects seen in HeLa cells transfected with *Cav1* siRNA, which showed an increased cell surface area and impaired chemotaxis (supplementary material Fig. S4F). Conversely, overexpression of GFP-Cav1 in HeLa cells decreased cell spreading (supplementary material Fig. S4E).

Finally, 1 hour pretreatment of cells with the Rac1 inhibitors EHT1864 (50 μM) (Shutes et al., 2007) or NSC23766 (100 μM) prior to cell spreading completely impaired the enhanced cell spreading that followed the depletion of Cav1, suggesting that the enhanced spreading that follows the loss of Cav1 expression is due to increased Rac1 activity (Fig. 3D,E; supplementary material Fig. S4E). Similarly, siRNA-mediated reduction of Rac1 expression impaired cell spreading, as measured by ECIS (supplementary material Fig. S4G,H). Thus, as Rac1 targeting to FAs is driven by β-Pix (ten Klooster et al., 2006), subsequent recruitment of Cav1 could serve to negatively regulate Rac1 signalling to allow cell polarization.

Cav1 regulates Rac1 ubiquitylation

Because Cav1 depletion promotes Rac1-dependent cell spreading, we analyzed GTP loading of Rac1 in control cells and HeLa cells treated with *Cav1* siRNA, using the Pak-Crib pull-down assay (ten Klooster et al., 2006). Surprisingly, the levels of not only Rac1-GTP, but also total Rac1 protein were increased in HeLa cells transfected with *Cav1* siRNA (Fig. 4A). To further corroborate this result, we analyzed Rac1 levels in $Cav1^{-/-}$ MEFs. Also in these cells, we found that the levels of total Rac1 and its GTP-bound form were increased to a similar degree compared with the levels in the wild-type MEFs (Fig. 4B).

The Pak-Crib pull-down is performed in NP40-containing lysis buffer. To exclude the possibility that our interpretation was obscured as a result of a change in the solubility of a fraction of endogenous Rac1, Rac1 protein levels were analyzed in control cells and HeLa cells treated with *Cav1* siRNA that were lysed directly in SDS sample buffer (Fig. 4C; supplementary material Fig. S2A). Under these conditions, Rac1 protein levels were also found to increase upon depletion of Cav1 by *Cav1* siRNA. This shows that this effect involves the total pool of cellular Rac1. Moreover, two independent Cav1 short hairpin RNAs (shRNAs), which were used as a control for possible off-target effects of the *Cav1* siRNA, were also found to increase Rac1 protein expression upon silencing of Cav1 (supplementary material Fig. S2C). Similarly, Rac1 protein expression is increased in HUVEC transfected with *Cav1* siRNA and in $Cav1^{-/-}$ MEFs, which furthermore shows that the increased expression of Rac1 upon loss of Cav1 is not cell-type specific (Fig. 4C). Unlike Rac1, the protein expression levels of RhoA or CDC42 were not affected by loss of Cav1 (Fig. 4C). Finally, although Cav1 can associate with RhoA (Fig. 1A), RhoA-GTP levels have been described to decrease in the absence of Cav1 (Grande-Garcia et al., 2007); this underscores that the Cav1-dependent regulation of RhoA markedly contrasts with Cav1 regulation of Rac1.

These data suggest that Cav1 affects Rac1 signalling output by regulating its protein-expression level. We therefore analyzed

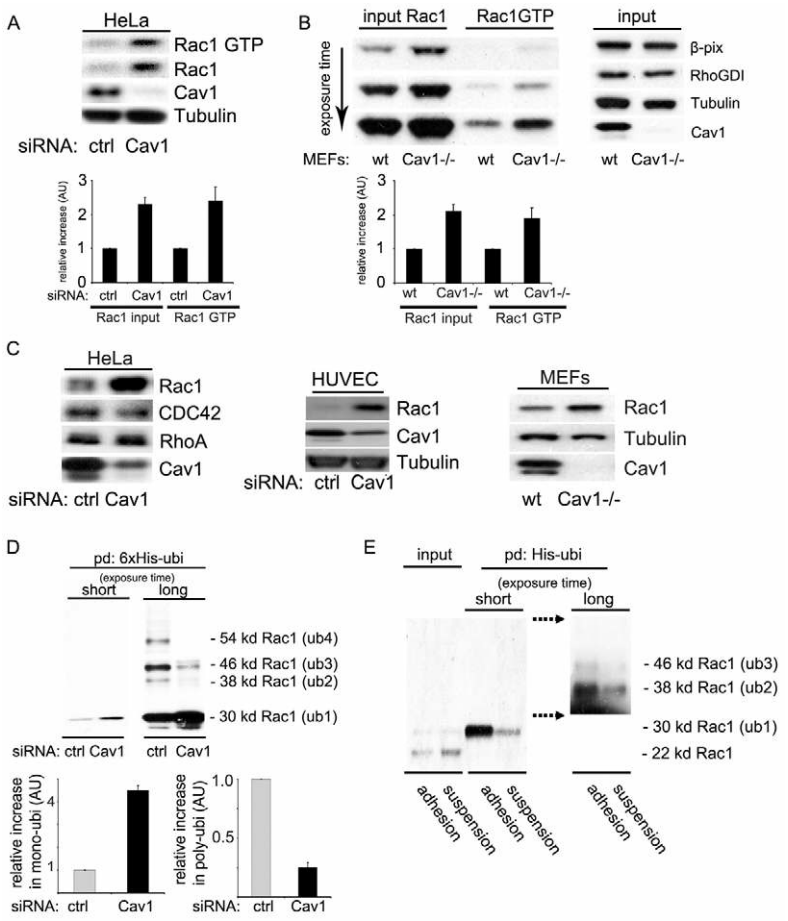

Fig. 4. Loss of Cav1 increases total and activated Rac1 levels. (**A**) Rac1 activation was assayed by biotinylated Pak-Crib peptide-based pull down using lysates of control cells and HeLa cells transfected with *Cav1* siRNA. The bar diagram depicts the relative increase in Rac1 expression and activation levels in cells treated with *Cav1* siRNA compared with control cells, as determined by quantification of western blots (n=3). Loss of Cav1 is associated with an approximately twofold increase in total and activated levels of Rac1. (**B**) Rac1 activation and expression were assayed by biotinylated Pak-Crib peptide-based pull down in lysates of wild-type (wt) and Cav1$^{-/-}$ MEFs. The bar diagram depicts the relative increase in Rac1 expression and activation levels in Cav1-depleted Cav1$^{-/-}$ fibroblasts compared with parental cells, as determined by quantification of blots (n=3). Like siRNA-based depletion of Cav1, loss of Cav1 in Cav1$^{-/-}$ MEFs is associated with an approximately twofold increase in total and activated levels of Rac1. (**C**) SDS lysates of control cells and cells transfected with *Cav1* siRNA were analyzed for protein levels of Rac1, CDC42 and RhoA. Rac1 levels in SDS lysates were also determined in HUVEC cells transfected with *Cav1* siRNA and in Cav1$^{-/-}$ MEFs. (**D**) Endogenous ubiquitylated Rac1 was isolated by cobalt-bead-based pull down from lysates of control cells and HeLa cells transfected with *Cav1* siRNA co-transfected with 6×His-myc-tagged ubiquitin. Two exposures of the western blot are shown to underscore the increase in mono-ubiquitylated endogenous Rac1 (short exposure, left) and the reduction in polyubiquitylated Rac1 (long exposure, right) in cells transfected with the *Cav1* siRNA. The relative differences in mono- and poly-ubiquitylation were quantified by densitometry (n=3) and are indicated in the bar graphs. In addition, the sizes of the various ubiquitylated forms of Rac1 (Rac1 ~22 kDa; Rac1-Ub ~30 kDa; Rac1-Ub2 ~38 kDa; Rac1-Ub3 ~46 kDa and Rac1-Ub4 ~54 kDa) are indicated. (**E**) Analysis of adhesion-dependent mono-ubiquitylation of endogenous Rac1 in HeLa cells. Prior to lysis and isolation of ubiquitylated proteins, cells transfected with 6×His-myc-tagged ubiquitin were either seeded on fibronectin for 2 hours or kept in suspension. Western blotting following isolation of ubiquitylated proteins was used to detect mono-ubiquitylated Rac1 (short exposure, left) and polyubiquitylated Rac1 (long exposure, right), as detected by immunostaining with a Rac1 antibody.

whether depletion of Cav1 increases mRNA levels of Rac1. Real-time quantitative PCR (RQ-PCR) on cDNA from control cells and cells transfected with *Cav1* siRNA revealed no changes in the mRNA levels of either Rac1 or RhoA (supplementary material Fig. S2B). To test whether Cav1 plays a role in ubiquitylation and degradation of Rac1, control cells and cells transfected with Cav1 *siRNA* were co-transfected with His-tagged ubiquitin to isolate endogenous ubiquitylated Rac1 by a cobalt-bead-based approach (Fig. 4D). In contrast to control cells, siRNA-mediated depletion of Cav1 induced a fourfold accumulation of mono-ubiquitylated endogenous Rac1, which migrates at an apparent molecular weight of 30 kDa on SDS-PAGE. By contrast, the levels of polyubiquitylated Rac1 were reduced to approximately 25% in the absence of Cav1. Thus, Cav1 regulates polyubiquitylation and probably the consequent degradation of Rac1, which might explain the increase in Rac1 protein levels upon loss of Cav1 expression. As Rac1 degradation is driven by the proteasome (Lerm et al., 1999; Doye et al., 2002; Boyer et al., 2006; Visvikis et al., 2008), we tested whether treating wild-type and Cav1$^{-/-}$ MEFs with proteasome inhibitors would level the increase in Rac1 protein levels in Cav1-depleted cells. However, these experiments were inconclusive, because 4 hours of treatment with a proteasome inhibitor is toxic to the cells, precluding further analysis.

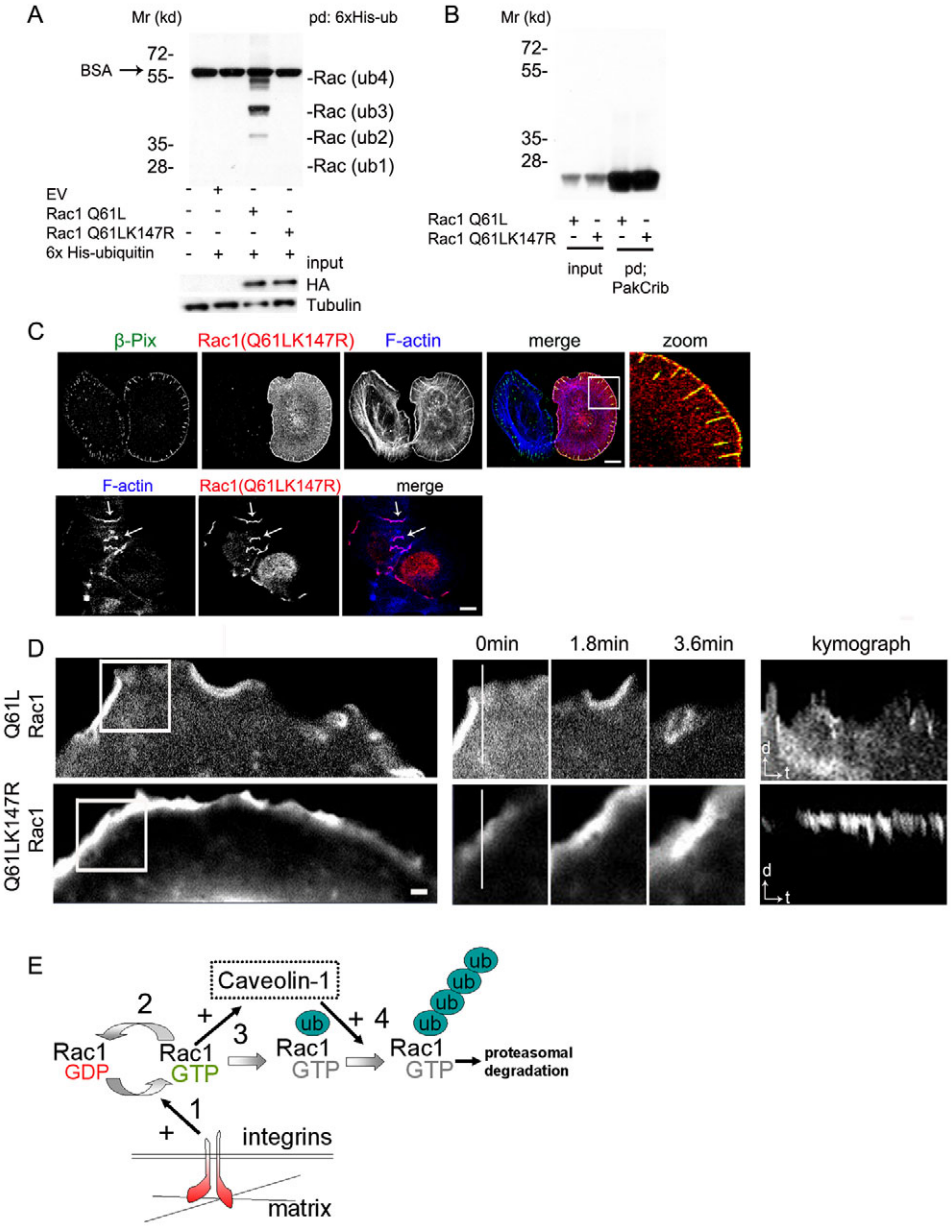

Fig. 5. Ubiquitylation is not required for Rac1 targeting. (**A**) Ubiquitylation of HA-tagged Rac1Q61L or Rac1Q61LK147R was analyzed as in Fig. 4. Immunoblots were stained for HA to detect ubiquitylated Rac1. (**B**) Effector binding to Rac1Q61L and Rac1Q61LK147R was assayed with a Pak-Crib peptide-based pull down. Ubiquitylation of activated Rac1 is not required for binding to the PAK-Crib domain. (**C**) Confocal imaging of immunostaining showing that Rac1Q61K147R localizes to β-Pix-positive FAs (upper panels) and to membrane ruffles, as identified by F-actin (lower panels, arrows). Scale bar: 10 μm. (**D**) Still images and corresponding kymograph analysis, derived from the indicated line [*t* (time), 25 seconds; *d* (distance), 1 μm] obtained by live-cell imaging of YFP-tagged Rac1Q61L and mCherry-tagged Rac1Q61LK147. (**E**) A model for the regulation of Rac1 activation and inactivation. Integrin-ligand interactions promote Rac1 activation (1), which, together with β-Pix, induces the accumulation of Rac1 at peripheral adhesions. Rac1 inactivation is balanced by (2) GAP-stimulated GTP hydrolysis, as well as by a Rac1 ubiquitylation pathway (3), which is regulated by Cav1 (4). Loss of Cav1 is associated with reduced polyubiquitylation of Rac1 and with an accumulation of mono-ubiquitylated Rac1, as well as activated and total Rac1.

Because integrins mediate Rac1 activation (Price et al., 1998) and adhesion regulates the Rac1-Cav1 interaction (Fig. 2E), we tested whether loss of integrin function would also affect the ubiquitylation of Rac1. We found that, in cells kept in suspension for 2 hours, mono-ubiquitylation and polyubiquitylation of endogenous Rac1 were inhibited, relative to its ubiquitylation in adherent cells (Fig. 4E). Thus, integrins regulate Rac1 activation (Price et al., 1998) and ubiquitylation.

Rac1 ubiquitylation regulates peripheral Rac1 dynamics

Previous studies using activation of endogenous Rac1 by CNF1 or using expression of activated Rac1 mutants have clearly demonstrated the positive correlation between Rac1 activation, its ubiquitylation and its consequent degradation (Doye et al., 2002; Pop et al., 2004; Visvikis et al., 2008). However, the relevance of ubiquitylation to Rac1 localization or signalling has not been previously investigated. Whereas constitutively active Rac1Q61L shows extensive polyubiquitylation, an activated mutant in which lysine 147 is mutated (Rac1Q61LK147R) (Visvikis et al., 2008) is not ubiquitylated at all (Fig. 5A). Activated Rac1 and the K147 mutant bind equally well to the CRIB domain of PAK, and localize readily to β-Pix-positive FAs and membrane ruffles (Fig. 5B,C). Interestingly, Rac1-induced recruitment of Cav1 to peripheral adhesions is not driven by (mono-)ubiquitylation of Rac1, as Rac1Q61LK147R is still found to promote Cav1 localization at such adhesions (supplementary material Fig. S2D).

These data therefore suggest that neither the targeting of Rac1 nor its interaction with the effector protein PAK requires its ubiquitylation. In line with this, expression of the Rac1Q61LK147R protein, like Rac1Q61L, stimulated peripheral membrane ruffling. However, live-cell analysis of these peripheral membranes showed that the Rac1Q61LK147R protein markedly accumulates at the periphery of the cell, compared with the Rac1Q61L protein (Fig.

5D; supplementary material Movies 4 and 5). Moreover, activated Rac1Q61L was seen in regions near and in ruffles, whereas the Rac1Q61LK147 protein localized to a more stable and narrow region near the peripheral membrane. Similarly, live-cell analysis of a mCherry-Rac1wt K147R mutant showed that this protein also localized more prominently to peripheral ruffles compared with mCherry-Rac1 wild type (supplementary material Fig. S2F). These data suggest that ubiquitylation of Rac1 neither impairs its targeting to the periphery of the cell nor affects Rac1 binding to effector proteins, but is important for Rac1 dynamics in peripheral membrane ruffles.

Discussion

The cycling of Rho-like GTPases, regulated by GEFs and GAPs, is generally assumed to be the principal mechanism by which cells ensure proper activation and inactivation of these GTPases at the correct time and location (Bos et al., 2007; Rossman et al., 2005). However, there is increasing evidence that regulation of Rho GTPase signalling by ubiquitylation and degradation occurs as well. Whereas the initial studies in this field were mainly based on the use of the Rho-GTPase-activating toxin CNF1, the identification of the RhoA ubiquitin-ligase Smurf1 has generated novel insights into the role of GTPase ubiquitylation in the regulation of cell polarity. Smurf1 is recruited to cellular protrusions by the atypical protein kinase zeta, where it locally regulates RhoA levels (Wang et al., 2003), cell protrusion and cell migration (Sahai et al., 2007). This supports the concept that localized degradation might represent one of the mechanisms to regulate polarized GTPase activation (Kraynov et al., 2000) and, ultimately, directional cell migration.

In contrast to RhoA, the cellular components regulating the degradation of Rac1 have not yet been identified. Previous studies, based on CNF1-induced activation and degradation of Rac1, have underscored the relevance of the hypervariable domain in its C terminus to degradation (Lanning et al., 2004; Pop et al., 2004). In line with the high sequence diversity in this region between, otherwise very homologous, Rac isoforms, it was shown that CNF1-induced degradation is isoform specific and can in fact be transferred by exchanging the hypervariable domain among Rac1 isoforms (Pop et al., 2004). However, the site of ubiquitylation in Rac1, Lys147, does not reside in the C terminus, but is located more upstream in the protein (Visvikis et al., 2008). Thus, the C-terminal domain of Rac1 mediates a function and/or interaction that allows ubiquitylation further upstream in the protein. Our current findings suggest that the interaction between Rac1 and Cav1, mediated by the Rac1 hypervariable C-terminal domain, is part of an adhesion-regulated mechanism that controls Rac1 ubiquitylation and degradation.

The Rac1 C terminus was initially found to control Rac1 subcellular targeting mediated by its polybasic nature and the C-terminal lipid moiety (Joseph et al., 1994; ten Klooster and Hordijk, 2007). More recently, several studies from our group and others have established that the Rac1 C-terminal domain not only interacts with charged lipids in the membrane, but also selectively associates with a number of proteins involved in Rac1 signalling (Modha et al., 2008; ten Klooster et al., 2006; ten Klooster et al., 2007; van Hennik et al., 2003). We previously showed that the Rac1 and CDC42 GEF β-Pix binds the Rac1 C terminus and recruits Rac1 to leading edge FAs, one of the cellular locations of activated Rac1 (ten Klooster et al., 2006). In this present study, we show that activated Rac1, in turn, recruits Cav1 to peripheral FAs. This was observed following ectopic expression of Rac1Q61L and following activation of endogenous Rac1 in epithelial and endothelial cells, either using the CNF1 toxin or through the induction of cell spreading.

CNF1 treatment of the cells induced a phenotype resembling that induced by activated Rac1. However, because CNF1 also activates RhoA, we analyzed the contribution of RhoA signalling to Cav1 accumulation at FAs. Neither the activation of endogenous RhoA by MT depolymerization nor the transfection of an activated mutant of RhoA mimicked the CNF1- or activated-Rac1-induced accumulation of Cav1 at FAs. Similarly, inhibition of ROCK, an effector of activated RhoA, did not prevent Cav1 from accumulating at peripheral adhesions, despite a significant change in the distribution of these structures (supplementary material Fig. S3D). Thus, RhoA-ROCK signalling does not contribute to the CNF1- or Rac1-induced translocation of Cav1. Cav1 recruitment to FAs is also independent of MTs, which suggests that the Cav1 is recruited from other regions within the plasma membrane or from the Golgi (Conrad et al., 1995). Cav1 has been suggested previously to associate with integrins (Wary et al., 1998), which is in line with our data showing that integrin-mediated adhesion, like activation of Rac1 by CNF1, targets Cav1 to FAs. Moreover, cell adhesion stimulated the interaction between Rac1 and Cav1, suggesting that Rac1 and integrins cooperate in the targeting of Cav1 to FAs, where Cav1 functions in integrin- and Rac1-mediated signalling. Finally, several reports have suggested that Cav1 tyrosine phosphorylation localizes Cav1 to FAs. However, these findings were questioned when it was shown that the commonly used mouse antibody against tyrosine-phosphorylated Cav1 cross-reacted with tyrosine-phosphorylated paxillin, which also resides in FAs (Hill et al., 2007). For this reason, we did not pursue immunostaining for pYCav1, but rather stained for endogenous total Cav1. We could not detect significant levels of tyrosine-phosphorylated Cav1 on western blots of cell lysates, unless cells were pretreated with pervanadate. This pYCav1 also associated with the Rac1 C-terminal domain, indicating that tyrosine phosphorylation did not interfere with Rac1 binding. We also did not find detectable levels of pYCav1 in Rac1 C-terminal pull-down assays (data not shown), which indicates that there is no preferential binding of phosphorylated Cav1 to Rac1. Similarly, a phospho-deficient mutant of Cav1 could bind to Rac1, but was inefficiently targeted to FAs, even in the presence of an activated mutant of Rac1, suggesting that Rac1 activity cooperates with a phosphorylation-dependent mechanism to accumulate Cav1 at FAs. Previously, tyrosine-phosphorylated Cav1 has been implicated in focal adhesion kinase stabilization, RhoA activation and FA turnover (Goetz et al., 2008; Joshi et al., 2008). Moreover, Cav1 tyrosine phosphorylation has been suggested to promote membrane order in FAs (Gaus et al., 2006). Thus, although phosphorylation of Cav1 is not crucial to Rac1 association, it appears important for Cav1 targeting to FAs and FA stability and, as such, does play an important role in cell spreading and cell motility.

In polarized cells, most of the Cav1 localizes to the rear (Fig. 2A,B), near areas of elevated contractility. This polarized distribution is in good agreement with its positive regulatory role in RhoA signalling (Grande-Garcia et al., 2007; Joshi et al., 2008). Moreover, we found that loss of Cav1 does not alter the protein levels of RhoA, the activity of which is crucial to myosin-based contractility at the back of migrating cells. Given the role of Cav1 in Rac1 degradation, the concept of localized GTPase degradation in polarized cells that has been proposed for RhoA (Wang et al., 2003) might also apply to Rac1. Rac1 activity is high in the leading

edge of polarized cells, away from the majority of Cav1 protein, but our data suggest that a portion of Cav1 is recruited to leading-edge FAs as a result of local activation of Rac1. The high levels of Cav1 at the back of polarized cells might serve to maintain Rac1 activity at a low level, locally preventing protrusive activity (Worthylake and Burridge, 2003).

The finding that reduction of Cav1 expression results in the accumulation of (activated) non-ubiquitylated Rac1 and mono-ubiquitylated Rac1, but not poly-ubiquitylated Rac1, suggests that Cav1 plays a specific role in the regulation of polyubiquitylation and subsequent degradation of Rac1. For some proteins, such as Ras and the epidermal growth factor receptor, mono-ubiquitylation is a trigger for internalization and signal transduction, for example, at endosomes (Haglund et al., 2003; Jura et al., 2006; Mukherjee et al., 2006). It is currently unclear at what subcellular location Rac1 ubiquitylation and degradation occurs. Cav1 has been implicated in integrin-dependent internalization of Rac1-containing membrane domains, which is accompanied by a loss of Rac1-effector interactions (del Pozo et al., 2004; del Pozo et al., 2005). Because loss of Cav1 does not impair mono-ubiquitylation of Rac1, this step might occur prior to Cav1-mediated internalization and subsequent polyubiquitylation. Whether mono-ubiquitylation of Rac1 mediates Rac1 internalization is currently the subject of investigation.

The cycling of Rho-like GTPases, regulated by GEFs and GAPs, is generally assumed to control localized activation and inactivation of these GTPases (Bos et al., 2007). Our current findings indicate that, in the absence of Cav1, the levels of activated, endogenous Rac1 remain elevated over prolonged periods of time (i.e. 48 hours). In line with this, interfering with this pathway by reducing Cav1 results in the accumulation of activated Rac1 and induction of a Rac1 phenotype, that is, increased cell spreading, loss of polarity and consequently reduced directional migration. This suggests that endogenous Rac1GAP activity is not sufficient to counteract this accumulation of GTP-loaded Rac1, indicating that the degradation of activated Rac1 represents an important complementary mechanism to control Rac1 signalling. Interestingly, a similar finding was recently reported for RhoA and its ubiquitylation by a Cullin-3–BACURD complex, as siRNA-mediated knockdown of Cullin-3 increased the levels not only of total RhoA, but also of its activated GTP-bound form (Chen et al., 2009).

In conclusion, our previous and current data suggest the following model (Fig. 5E). In polarized cells, integrin-mediated adhesion recruits the GEF β-Pix to leading-edge FAs (ten Klooster et al., 2006), followed by β-Pix-mediated recruitment and local activation of Rac1 at FAs. Rac1 activity recruits Cav1 to FAs and integrin activation promotes the Rac1-Cav1 association. Cav1 subsequently controls efficient termination of Rac1 signalling by regulating Rac1 polyubiquitylation and degradation. Future experiments will be aimed at defining the subcellular localization of the different steps in the Rac1 ubiquitylation pathway as well as identifying the relevant E3 ligase. The polarized distribution of Cav1 and its role in Rac1 ubiquitylation provide further support for the concept of localized protein degradation in polarized cells.

Materials and Methods

Antibodies and reagents

The following antibodies were used: anti-caveolin-1 (610493), anti-caveolin-2 (610684), anti-p(Y14) caveolin-1 (610059), anti-paxillin (610619) (all from BD Bioscience), anti-Rac1 (clone 23A8) and anti-β-Pix (AB3829) (both from Millipore), anti-RhoA (sc-418) and I1PP2A (Santa Cruz), anti-pY118 paxillin (44-722G) (Invitrogen), anti-GFP (JL-8; Clontech), anti-c-myc (Zymed), F-actin stained with rhodamine-labelled phalloidin (Invitrogen). The Rac1 inhibitors EHT1864 and NSC23766 were obtained from Sigma and Calbiochem, respectively. Confocal imaging of immunostained samples and live-cell imaging were done using a ZEISS LSM510 Meta system in combination with ZEISS Zen software for analysis and processing. All data are representative of three or more experiments, unless otherwise indicated. Movies are representative of at least 3-10 cells, analyzed individually.

Cell culture

HeLa cells were maintained in IMDM (BioWhittaker) containing 10% heat-inactivated FCS (Bodinco), 2 mM L-glutamine and penicillin-streptomycin (all purchased from PAA Cell Culture Company). Cells were passed by trypsinization. HUVEC were obtained from Lonza and cultured in EGM2 medium (Lonza) prepared according to the manufacturer's instructions. $Cav1^{-/-}$ knockout (ATCC-CRL-2752) and parental wild-type (ATCC-CRL-2753) MEFs were obtained from ATCC and cultured in DMEM containing 10% heat-inactivated FCS (Bodinco), 2 mM L-glutamine and penicillin-streptomycin. All cells were grown at 37°C in a humidified atmosphere containing 5% CO_2.

Cell transfection and DNA constructs

HeLa cells were transiently transfected with FuGENE (Roche), as described by the manufacturer. Briefly, 1 μg DNA was mixed with 6 μl FuGENE in 100 μl Optimem (51985026) (Invitrogen) and incubated for 30 minutes at room temperature, after which the transfection mix was applied to 50% confluent cells. The following constructs were used: GFP-Cav1 (a kind gift from Martin A. Schwartz, University of Virginia, Charlottesville, VA); GFP-CavY14F (constructed by site-directed mutagenesis; Stratagene); GST-Rac and GST-RacΔC (a kind gift from Reza Ahmadian, European Molecular and Cell Biology Laboratory, Heidelberg, Germany) (Haeusler et al., 2003) and GST-Cav1 (kindly provided by Elsa Regan-Klapisz, Utrecht University, The Netherlands). 6×His-myc-tagged ubiquitin expression plasmid, originally from Ron R. Kopito (Ward et al., 1995), was kindly provided by Jacques Bertoglio (Inserm U749, France). myc-Cav1 and myc-Cav1Δ80-100 constructs were kindly provided by Richard G. W. Anderson (Machleidt et al., 2000). pCMV-myc-tagged Rac1Q61L was subcloned into pCruz HA-tagged expression vector (sc-5045), after which Rac1Q61LK147R was generated by site-directed mutagenesis (Stratagene). In parallel, Rac1Q61L and Rac1 Q61LK147R were subsequently cloned in pE-YFP-(C1)- and m-Cherry (C1)-tagged constructs. The same protocol has been used for wild-type Rac1. CNF1 was isolated as previously described (Schmidt et al., 1997). Cells were incubated with 500 ng/ml purified GST-CNF1 toxin, as indicated.

Design and transfection of siRNA oligomers

HeLa cells (4.10e5) were passed by trypsinization in a 10 cm dish, neutralized with complete IMDM and cultured overnight in Opti-mem I medium (Invitrogen). After 18 hours, siRNA transfection mix containing siRNA primers (87 μl of 20 μM) and Oligofectamine (87 μl) was prepared in Opti-mem I medium according the manufacturer's protocol (Invitrogen) and incubated for 30 minutes at room temperature. During this incubation, the Opti-mem I medium was replaced with IMDM complete medium. Transfection medium was removed 24 hours after transfection by replacing the culture medium with complete IMDM. The following chemically synthesized, double-stranded siRNAs, with 19-nucleotide duplex RNA and 2- nucleotide 3′-dTdT, purchased from Eurogentec in non-modified and desalted form, were used. Caveolin-1 siRNA primers AAUCUCAAUCAGGAAGCUC (5′-3′) and GAGCUUCCUGAUUGAGAUU (5′-3′) (Beardsley et al., 2005). Rac1 siRNA primers GAGGAAGAGAAAAUGCCU (5′-3′) and CAGGCAUUUUCUCUU-CCUC (5′-3′) (Noritake et al., 2004). As a non-specific control in this study, we used an siRNA against a luciferase reporter gene: CGUACGCGGAAUACUUCGA (5′-3′) and GCAUGCGCCUUAUGAAGCU (5′-3′).

Lentiviral shRNAi silencing

Lentiviral shRNA constructs from the TRC and Sigma Mission library (Root et al., 2006) were obtained from Sigma-Aldrich (St Louis, MI). The human Cav1-specific constructs used were: TRCN0000007999-8002 (called A6-A9) and TRCN0000011218 (called A5). The SHC002 scrambled shRNA construct (Sigma-Aldrich) was used as a negative control. All shRNA constructs were in the pLKO.1 vector backbone. shRNA-expressing lentiviral particles were prepared by transfection of HEK293T cells with pLKO.1 shRNA plasmid, together with the pMD2.G, pMDLg/RRE and pRSV-Rev third-generation HIV-1 packaging plasmids (Hope et al., 1990; Dull et al., 1998; obtained through Addgene, Cambridge, MA), using FuGENE HD (Roche 04709713001, Almere, The Netherlands). Virus-containing medium was collected for 3 days post-transfection and cleaned up by filtration through a 0.45 μm polyvinylidene fluoride filter unit (Millipore SLHV033RS, Amsterdam, The Netherlands). Virus was further purified and concentrated 60- to 80-fold by centrifugation for 65 minutes at 13,000 ***g*** in a Beckman SW32.1 rotor (Beckman-Coulter, Mijdrecht, The Netherlands). shRNA-expressing virus titer was determined by functional titration on target cells using the pLKO.1 puromycin selection marker. The lowest amount of virus giving >90% puromycin resistance was taken to represent a multiplicity of infection (MOI) of 2-3. Target cells were infected using this MOI and, 24 hours after the addition of virus, medium was

refreshed. Cells were harvested after 48 hours and Cav1 knockdown was determined using western blot.

RNA extraction, reverse transcription and RQ-PCR

Total cellular RNA from control and Cav1-knockdown cells was extracted with RNA-Bee (Bioconnect), according to the manufacturer's instructions. cDNA was synthesized using 1 μg total RNA according to the Europe Against Cancer (EAC) guidelines (Gabert et al., 2003). Primers for RAC1 and RHOA were designed using Primer Express 1.5 (Applied Biosystems, Foster City, CA) and OLIGO 6 (Molecular Biology Insights Inc, Cascade, CO) on the basis of published gene sequences (http://www.ncbi.nlm.nih.gov/). Amplicons spanned an intron of at least 500 base pairs. Primers were synthesized by Eurogentec (Liege, Belgium). Primer combination for RAC1: forward primer 5′-CCTGATGCAGGCCATCAAG-3′; reverse primer 5′-AGTAGGGATATATTCTCCAGGAAATGC-3′. Primer combination for RHOA: forward primer 5′-GGACTCGGATTCGTTGCCT-3; reverse primer 5′-CCATC-ACCAACAATCACCAGTT-3′. Primer combination for β-glucuronidase (GUS): forward primer 5′-GAAAATATGTGGTTGGAGAGCTCATT-3′; reverse primer 5′-CCGAGTGAAGATCCCCTTTTTA-3′. RQ-PCR was performed in an Applied Biosystems 7900HT fast real-time PCR system (Applied Biosystems, Foster City, CA). Reactions were carried out in 25 μl containing 12.5 μl SYBR Green PCR Master Mix (Applied Biosystems), 300 nM forward and reverse primer, 5 μl cDNA (100 ng RNA equivalents). PCR started with 10 minutes at 95°C followed by 50 cycles of 15 seconds at 95°C and 60 seconds at 60°C. The specificity of all PCR products was determined by melt curve analysis. To correct for differences in the amount of total RNA input and for reverse transcriptase efficiency, the quantity of the RAC1 and RHOA transcripts was normalized to the amount of GUS gene transcripts.

Pull-down assays

Peptide pull-down assays were performed as described previously (ten Klooster et al., 2006). In short, each assay was performed with 5 μg of indicated biotin-labelled peptide and 25 μl streptavidin-coated beads (Sigma-Aldrich) in NP-40 lysis buffer (50 mM Tris-HCl, 150 mM NaCl, 10 mM $MgCl_2$, 10% glycerol, 1% NP-40). All peptides were fused to a protein transduction domain sequence, YARAAARQARA, that was also used as a control in the pull-down experiments (van Hennik et al., 2003). GST-fusion proteins were purified from BL21 bacteria as described (ten Klooster et al., 2006), after which 100 μg of indicated GST-fusion constructs was used in each pull down. Rac1 activation was assayed by a CRIB-peptide pull-down approach, as previously described (Price et al., 2003). Mass spectrometry analysis for the identification of Cav1 was done as described (Kanters et al., 2008).

Peptide synthesis

Peptides were synthesized on a peptide synthesizer (Syro II) using Fmoc solid-phase chemistry. Peptides encoded a biotinylated protein transduction domain (biotin-YARAAARQARAG) (Ho et al., 2001) followed by the 10 amino acids preceding the CAAX domain for all used Rho GTPase peptides. The sequences of Rac1 (P-A) and the Rac1 (RKR-AAA) mutants are, respectively, CAAAVKKRKRK and CPPPVKKAAAK. The biotinylated protein transduction domain of the cavtratin peptide (Gratton et al., 2003) was followed by 20 amino acids corresponding to the scaffolding domain (amino acids 82-101) of Cav1: DGIWKASFTTFTVTKYWFYR.

Rac1 ubiquitylation assay

To detect endogenous, ubiquitylated Rac1 in HeLa cells, cells were transfected with 6×His-myc-tagged ubiquitin. 24 hours after transfection, cells were washed with PBS (containing Mg^{2+} and Ca^{2+}) at room temperature and lysed for 5 minutes in urea buffer (20 mM Tris-HCl, pH 7.5, 200 mM NaCl, 10 mM imidazole, 0.1% Triton X-100 in 8 M urea). Cells were scraped, collected and incubated for 5 minutes at 37°C and centrifuged for 5 minutes at 11,000 ***g***, after which the supernatant was incubated with 25 μl prewashed, blocked (1 hour at room temperature with 200 μg/ml BSA) TALON beads (Clontech) at room temperature for 1 hour while rotating. Beads were washed five times with urea buffer and resuspended in SDS sample buffer. Endogenous, ubiquitylated Rac1 was detected by western blotting for Rac1.

Cell migration

Serum-starved control cells and HeLa cells transfected with *Cav1* siRNA were seeded 48 hours after transfection in fibronectin-coated 6.5 mm, 5 μm pore Transwell (100,000 cells/well) plates (Corning Costar, Cambridge, MA). Cells were subsequently allowed to migrate for 4 hours towards IMDM with 10% FCS in the lower compartment. Cells in the upper compartment were removed with a cotton swab, and the cells in the lower compartment were fixed and stained with Hoechst (Invitrogen). The number of migrated cells was determined by manual counting of fluorescent-stained nuclei.

Electrical resistance measurements

For ECIS-based cell-spreading experiments (ten Klooster et al., 2006), ECIS electrodes (8W10E; Applied Biophysics) were coated with 10 μg/ml fibronectin (Sigma) in PBS for 1 hour at 37°C. 200,000 HeLa cells transfected with siRNA were seeded per well in 400 μl IMDM containing 10% FCS, L-glutamine and penicillin-streptomycin. Cell spreading was monitored by measuring the impedance for up to 4 hours.

The authors thank Martin Schwartz for GFP-Cav-1, Elsa Regan-Klapisz for GST-Cav-1, Reza Ahmadian for GST-Rac1, Jacques Bertoglio for 6×His-myc-ubiquitin, Richad G. W. Anderson for myc-tagged Cav1 and Cav1 Δ80-100, and John Collard for Rac3 C-terminal peptide and for critical reading of the manuscript.

Supplementary material available online at
http://jcs.biologists.org/cgi/content/full/123/11/1948/DC1

References

Beardsley, A., Fang, K., Mertz, H., Castranova, V., Friend, S. and Liu, J. (2005). Loss of caveolin-1 polarity impedes endothelial cell polarization and directional movement. *J. Biol. Chem.* **280**, 3541-3547.

Bernards, A. and Settleman, J. (2004). GAP control: regulating the regulators of small GTPases. *Trends Cell. Biol.* **14**, 377-385.

Bershadsky, A. D., Ballestrem, C., Carramusa, L., Zilberman, Y., Gilquin, B., Khochbin, S., Alexandrova, A. Y., Verkhovsky, A. B., Shemesh, T. and Kozlov, M. M. (2006). Assembly and mechanosensory function of focal adhesions: experiments and models. *Eur. J. Cell Biol.* **85**, 165-173.

Bos, J. L., Rehmann, H. and Wittinghofer, A. (2007). GEFs and GAPs: critical elements in the control of small G proteins. *Cell* **129**, 865-877.

Boyer, L., Turchi, L., Desnues, B., Doye, A., Ponzio, G., Mege, J. L., Yamashita, M., Zhang, Y. E., Bertoglio, J., Flatau, G. et al. (2006). CNF1-induced biquitylation and proteasome destruction of activated RhoA is impaired in $Smurf1^{-/-}$ cells. *Mol. Biol. Cell* **17**, 2489-2497.

Chen, Y., Yang, Z., Meng, M., Zhao, Y., Dong, N., Yan, H., Liu, L., Ding, M., Peng, H. B. and Shao, F. (2009). Cullin mediates degradation of RhoA through evolutionarily conserved BTB adaptors to control actin cytoskeleton structure and cell movement. *Mol. Cell* **35**, 841-855.

Conrad, P. A., Smart, E. J., Ying, Y. S., Anderson, R. G. and Bloom, G. S. (1995). Caveolin cycles between plasma membrane caveolae and the Golgi complex by microtubule-dependent and microtubule-independent steps. *J. Cell Biol.* **131**, 1421-1433.

del Pozo, M. A., Alderson, N. B., Kiosses, W. B., Chiang, H. H., Anderson, R. G. and Schwartz, M. A. (2004). Integrins regulate Rac targeting by internalization of membrane domains. *Science* **303**, 839-842.

del Pozo, M. A., Balasubramanian, N., Alderson, N. B., Kiosses, W. B., Grande-Garcia, A., Anderson, R. G. and Schwartz, M. A. (2005). Phospho-caveolin-1 mediates integrin-regulated membrane domain internalization. *Nat. Cell. Biol.* **7**, 901-908.

DerMardirossian, C. and Bokoch, G. M. (2005). GDIs: central regulatory molecules in Rho GTPase activation. *Trends Cell. Biol.* **15**, 356-363.

Dovas, A. and Couchman, J. R. (2005). RhoGDI: multiple functions in the regulation of Rho family GTPase activities. *Biochem. J.* **390**, 1-9.

Doye, A., Mettouchi, A., Bossis, G., Clement, R., Buisson-Touati, C., Flatau, G., Gagnoux, L., Piechaczyk, M., Boquet, P. and Lemichez, E. (2002). CNF1 exploits the ubiquitin-proteasome machinery to restrict Rho GTPase activation for bacterial host cell invasion. *Cell* **111**, 553-564.

Dull, T., Zufferey, R., Kelly, M., Mandel, R. J., Nguyen, M., Trono, D. and Naldini, L. (1998). A third-generation lentivirus vector with a conditional packaging system. *J. Virol.* **72**, 8463-8471.

Enomoto, T. (1996). Microtubule disruption induces the formation of actin stress fibers and focal adhesions in cultured cells: possible involvement of the rho signal cascade. *Cell Struct. Funct.* **21**, 317-326.

Flatau, G., Lemichez, E., Gauthier, M., Chardin, P., Paris, S., Fiorentini, C. and Boquet, P. (1997). Toxin-induced activation of the G protein p21 Rho by deamidation of glutamine. *Nature* **387**, 729-733.

Gabert, J., Beillard, E., van der Velden, V. H., Bi, W., Grimwade, D., Pallisgaard, N., Barbany, G., Cazzaniga, G., Cayuela, J. M., Cave, H. et al. (2003). Standardization and quality control studies of 'real-time' quantitative reverse transcriptase polymerase chain reaction of fusion gene transcripts for residual disease detection in leukemia – a Europe Against Cancer program. *Leukemia* **17**, 2318-2357.

Gaus, K., Le Lay, S., Balasubramanian, N. and Schwartz, M. A. (2006). Integrin-mediated adhesion regulates membrane order. *J. Cell Biol.* **174**, 725-734.

Gingras, D., Gauthier, F., Lamy, S., Desrosiers, R. R. and Beliveau, R. (1998). Localization of RhoA GTPase to endothelial caveolae-enriched membrane domains. *Biochem. Biophys. Res. Commun.* **247**, 888-893.

Goetz, J. G., Joshi, B., Lajoie, P., Strugnell, S. S., Scudamore, T., Kojic, L. D. and Nabi, I. R. (2008). Concerted regulation of focal adhesion dynamics by galectin-3 and tyrosine-phosphorylated caveolin-1. *J. Cell Biol.* **180**, 1261-1275.

Grande-Garcia, A., Echarri, A., de Rooij, J., Alderson, N. B., Waterman-Storer, C. M., Valdivielso, J. M. and del Pozo, M. A. (2007). Caveolin-1 regulates cell polarization and directional migration through Src kinase and Rho GTPases. *J. Cell Biol.* **177**, 683-694.

Gratton, J. P., Lin, M. I., Yu, J., Weiss, E. D., Jiang, Z. L., Fairchild, T. A., Iwakiri, Y., Groszmann, R., Claffey, K. P., Cheng, Y. C. et al. (2003). Selective inhibition of tumor microvascular permeability by cavtratin blocks tumor progression in mice. *Cancer Cell* **4**, 31-39.

Haeusler, L. C., Blumenstein, L., Stege, P., Dvorsky, R. and Ahmadian, M. R. (2003). Comparative functional analysis of the Rac GTPases. *FEBS Lett.* **555**, 556-560.

Haglund, K., Di Fiore, P. P. and Dikic, I. (2003). Distinct monoubiquitin signals in receptor endocytosis. *Trends Biochem. Sci.* **28**, 598-603.

Hill, M. M., Scherbakov, N., Schiefermeier, N., Baran, J., Hancock, J. F., Huber, L. A., Parton, R. G. and Parat, M. O. (2007). Reassessing the role of phosphocaveolin-1 in cell adhesion and migration. *Traffic* **8**, 1695-1705.

Ho, A., Schwarze, S. R., Mermelstein, S. J., Waksman, G. and Dowdy, S. F. (2001). Synthetic protein transduction domains: enhanced transduction potential in vitro and in vivo. *Cancer Res.* **61**, 474-477.

Hope, T. J., Huang, X. J., McDonald, D. and Parslow, T. G. (1990). Steroid-receptor fusion of the human immunodeficiency virus type 1 Rev transactivator: mapping cryptic functions of the arginine-rich motif. *Proc. Natl. Acad. Sci. USA* **87**, 7787-7791.

Joseph, G., Gorzalczany, Y., Koshkin, V. and Pick, E. (1994). Inhibition of NADPH oxidase activation by synthetic peptides mapping within the carboxyl-terminal domain of small GTP-binding proteins. Lack of amino acid sequence specificity and importance of polybasic motif. *J. Biol. Chem.* **269**, 29024-29031.

Joshi, B., Strugnell, S. S., Goetz, J. G., Kojic, L. D., Cox, M. E., Griffith, O. L., Chan, S. K., Jones, S. J., Leung, S. P., Masoudi, H. et al. (2008). Phosphorylated caveolin-1 regulates Rho/ROCK-dependent focal adhesion dynamics and tumor cell migration and invasion. *Cancer Res.* **68**, 8210-8220.

Jura, N., Scotto-Lavino, E., Sobczyk, A. and Bar-Sagi, D. (2006). Differential modification of Ras proteins by ubiquitination. *Mol. Cell* **21**, 679-687.

Kanters, E., van Rijssel, J., Hensbergen, P. J., Hondius, D., Mul, F. P., Deelder, A. M., Sonnenberg, A., van Buul, J. D. and Hordijk, P. L. (2008). Filamin B mediates ICAM-1-driven leukocyte transendothelial migration. *J. Biol. Chem.* **283**, 31830-31839.

Kraynov, V. S., Chamberlain, C., Bokoch, G. M., Schwartz, M. A., Slabaugh, S. and Hahn, K. M. (2000). Localized Rac activation dynamics visualized in living cells. *Science* **290**, 333-337.

Lanning, C. C., Daddona, J. L., Ruiz-Velasco, R., Shafer, S. H. and Williams, C. L. (2004). The Rac1 C-terminal polybasic region regulates the nuclear localization and protein degradation of Rac1. *J. Biol. Chem.* **279**, 44197-44210.

Lerm, M., Schmidt, G., Goehring, U. M., Schirmer, J. and Aktories, K. (1999) Identification of the region of rho involved in substrate recognition by Escherichia coli cytotoxic necrotizing factor 1 (CNF1). *J. Biol. Chem.* **274,** 28999-29004.

Lin, M., DiVito, M. M., Merajver, S. D., Boyanapalli, M. and van Golen, K. L. (2005). Regulation of pancreatic cancer cell migration and invasion by RhoC GTPase and caveolin-1. *Mol. Cancer* **4**, 21.

Lynch, E. A., Stall, J., Schmidt, G., Chavrier, P. and D'Souza-Schorey, C. (2006). Proteasome-mediated degradation of Rac1-GTP during epithelial cell scattering. *Mol. Biol. Cell* **17**, 2236-2242.

Machleidt, T., Li, W. P., Liu, P. and Anderson, R. G. (2000). Multiple domains in caveolin-1 control its intracellular traffic. *J. Cell Biol.* **148**, 17-28.

Modha, R., Campbell, L. J., Nietlispach, D., Buhecha, H. R., Owen, D. and Mott, H. R. (2008). The Rac1 polybasic region is required for interaction with its effector PRK1. *J. Biol. Chem.* **283**, 1492-1500.

Mukherjee, S., Tessema, M. and Wandinger-Ness, A. (2006). Vesicular trafficking of tyrosine kinase receptors and associated proteins in the regulation of signaling and vascular function. *Circ. Res.* **98**, 743-756.

Munro, P. and Lemichez, E. (2005). Bacterial toxins activating Rho GTPases. *Curr. Top. Microbiol. Immunol.* **291**, 177-190.

Noritake, J., Fukata, M., Sato, K., Nakagawa, M., Watanabe, T., Izumi, N., Wang, S., Fukata, Y. and Kaibuchi, K. (2004). Positive role of IQGAP1, an effector of Rac1, in actin-meshwork formation at sites of cell-cell contact. *Mol. Biol. Cell* **15**, 1065-1076.

Pop, M., Aktories, K. and Schmidt, G. (2004). Isotype-specific degradation of Rac activated by the cytotoxic necrotizing factor 1. *J. Biol. Chem.* **279**, 35840-35848.

Price, L. S., Leng, J., Schwartz, M. A. and Bokoch, G. M. (1998). Activation of Rac and Cdc42 by integrins mediates cell spreading. *Mol. Biol. Cell* **9**, 1863-1871.

Price, L. S., Langeslag, M., ten Klooster, J. P., Hordijk, P. L., Jalink, K. and Collard, J. G. (2003). Calcium signaling regulates translocation and activation of Rac. *J. Biol. Chem.* **278**, 39413-39421.

Razani, B., Woodman, S. E. and Lisanti, M. P. (2002). Caveolae: from cell biology to animal physiology. *Pharmacol. Rev.* **54**, 431-467.

Ridley, A. J., Schwartz, M. A., Burridge, K., Firtel, R. A., Ginsberg, M. H., Borisy, G., Parsons, J. T. and Horwitz, A. R. (2003). Cell migration: integrating signals from front to back. *Science* **302**, 1704-1709.

Root, D. E., Hacohen, N., Hahn, W. C., Lander, E. S. and Sabatini, D. M. (2006). Genome-scale loss-of-function screening with a lentiviral RNAi library. *Nat. Methods* **3**, 715-719.

Rossman, K. L., Der, C. J. and Sondek, J. (2005). GEF means go: turning on RHO GTPases with guanine nucleotide-exchange factors. *Nat. Rev. Mol. Cell Biol.* **6**, 167-180.

Sahai, E., Garcia-Medina, R., Pouyssegur, J. and Vial, E. (2007). Smurf1 regulates tumor cell plasticity and motility through degradation of RhoA leading to localized inhibition of contractility. *J. Cell Biol.* **176**, 35-42.

Schmidt, G., Sehr, P., Wilm, M., Selzer, J., Mann, M. and Aktories, K. (1997). Gln 63 of Rho is deamidated by Escherichia coli cytotoxic necrotizing factor-1. *Nature* **387**, 725-729.

Shutes, A., Onesto, C., Picard, V., Leblond, B., Schweighoffer, F. and Der, C. J. (2007). Specificity and mechanism of action of EHT 1864, a novel small molecule inhibitor of Rac family small GTPases. *J. Biol. Chem.* **282**, 35666-35678.

ten Klooster, J. P. and Hordijk, P. L. (2007). Targeting and localized signalling by small GTPases. *Biol. Cell* **99**, 1-12.

ten Klooster, J. P., Jaffer, Z. M., Chernoff, J. and Hordijk, P. L. (2006). Targeting and activation of Rac1 are mediated by the exchange factor beta-Pix. *J. Cell Biol.* **172**, 759-769.

ten Klooster, J. P., Leeuwen, I., Scheres, N., Anthony, E. C. and Hordijk, P. L. (2007). Rac1-induced cell migration requires membrane recruitment of the nuclear oncogene SET. *EMBO J.* **26**, 336-345.

van Hennik, P. B., ten Klooster, J. P., Halstead, J. R., Voermans, C., Anthony, E. C., Divecha, N. and Hordijk, P. L. (2003). The C-terminal domain of Rac1 contains two motifs that control targeting and signaling specificity. *J. Biol. Chem.* **278**, 39166-39175.

Vastrik, I., Eickholt, B. J., Walsh, F. S., Ridley, A. and Doherty, P. (1999). Sema3A-induced growth-cone collapse is mediated by Rac1 amino acids 17-32. *Curr. Biol.* **9**, 991-998.

Vicente-Manzanares, M., Webb, D. J. and Horwitz, A. R. (2005). Cell migration at a glance. *J. Cell Sci.* **118**, 4917-4919.

Visvikis, O., Lores, P., Boyer, L., Chardin, P., Lemichez, E. and Gacon, G. (2008). Activated Rac1, but not the tumorigenic variant Rac1b, is ubiquitinated on Lys 147 through a JNK-regulated process. *FEBS J.* **275**, 386-396.

Wang, H. R., Zhang, Y., Ozdamar, B., Ogunjimi, A. A., Alexandrova, E., Thomsen, G. H. and Wrana, J. L. (2003). Regulation of cell polarity and protrusion formation by targeting RhoA for degradation. *Science* **302**, 1775-1779.

Ward, C. L., Omura, S. and Kopito, R. R. (1995). Degradation of CFTR by the ubiquitin-proteasome pathway. *Cell* **83,** 121-127.

Wary, K. K., Mariotti, A., Zurzolo, C. and Giancotti, F. G. (1998). A requirement for caveolin-1 and associated kinase Fyn in integrin signaling and anchorage-dependent cell growth. *Cell* **94**, 625-634.

Worthylake, R. A. and Burridge, K. (2003). RhoA and ROCK promote migration by limiting membrane protrusions. *J. Biol. Chem.* **278**, 13578-13584.

Zuluaga, S., Gutierrez-Uzquiza, A., Bragado, P., Alvarez-Barrientos, A., Benito, M., Nebreda, A. R. and Porras, A. (2007). p38alpha MAPK can positively or negatively regulate Rac-1 activity depending on the presence of serum. *FEBS Lett.* **581**, 3819-3825.